RSC Advances

ROYAL SOCIETY OF CHEMISTRY

www.rsc.org/advances

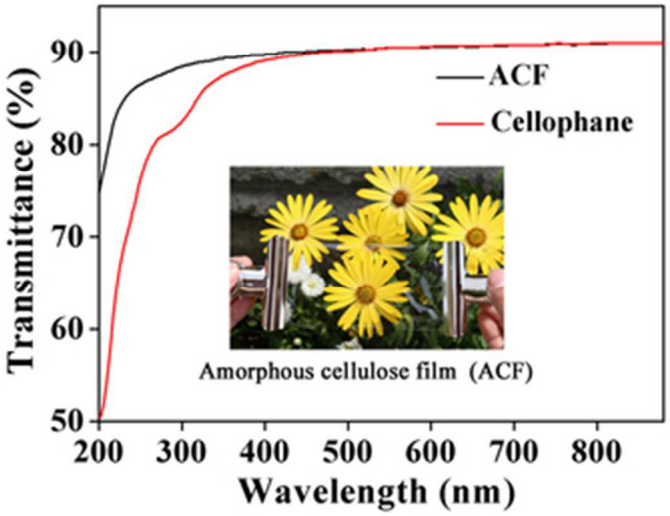

Graphic Abstract
34x24mm (300 x 300 DPI)

Preparation and Characterization of Transparent Amorphous Cellulose Film

Bo-xing Zhang, Jun-ichi Azuma, Hiroshi Uyama*

Department of Applied Chemistry, Graduate School of Engineering, Osaka University, Yamadaoka 2–1, Suita 565–0871, Japan

**Corresponding author E-mail: uyama@chem.eng.osaka-u.ac.jp; Fax: +81-6-6879-7367; Tel: +81-6-6879-7364*

Abstract: Amorphous cellulose film (ACF) was prepared from cellulose solution in lithium chloride (8 wt%)/*N,N*-dimethylacetamide by regeneration with acetone. The obtained ACF possessed dense, smooth surface, and excellent transparency. The X-ray diffraction results indicated that ACF was highly amorphous, which was further confirmed by solid-state ^{13}C-NMR and Fourier transform infrared (FT-IR) spectra. Tensile analysis implied that the elongation at break (23.9%) and maximum stress (157 MPa) of ACF that derived from Whatman CF11 fibrous cellulose were higher than those of cellophane (19.9% and 135 MPa, respectively). In addition, enzymatic hydrolysis of ACF and cellophane showed higher hydrolysis rate of the former (about 7 times higher than the latter), indicating outstanding environmental friendliness. This work provided a simple, less-destructive, and universal method to prepare transparent ACF, which may serve as a promising packaging material to replace cellophane.

Keywords: amorphous, cellulose film, enzymatic hydrolysis

Introduction

With the depleting fossil oil and ever-increasing environment concern, cellulose has recalled researchers' interest as a raw material over the last decades, due to its abundant resource, extraordinary renewability, biodegradability, and unique molecular structure.[1,2] Cellulose possesses great potential application in fiber, film, coating, and matrix of control-release systems, especially in food packaging area.[3] Nowadays, a commercial cellulose film (cellophane) is mainly produced by the viscose method. Another two methods (carbamate and Lyocell technologies) developed in recent years are also used to produce cellulose film.[3] However, most of cellulose films prepared by the existing methods possess cellulose II structure.

It is well known that cellulose is composed of a group of crystalline allomorphs (I, II, III_1, III_{11}, IV_1 and IV_{11}) and disordered (amorphous) structure with two polymorphs (I_α and I_β) in the cellulose I.[4] Molecular chains in amorphous cellulose are loosely arranged unlike tight compact in its crystalline counterpart, which would cause significant difference in some aspects, such as mechanical properties,[5] reaction kinetics[6] and enzymatic hydrolysis rate.[7-9] Some special application, such as enzyme screening and displaying material, could be developed with amorphous cellulose film (ACF). Meanwhile, it is of great importance to investigate the behaviors of ACF for better utilization of cellulose resource. However, most of cellulose films reported possess crystalline structure with cellulose II, since it is thermodynamically more stable than the other allomorphs.[3,10-12] In contrast, ACF with good performance was rarely reported, although many methods had been developed to prepare amorphous cellulose sample, such as ball milling,[13] hydrolysis of cellulose triacetate,[14] regeneration from cadmium ethylenediamine,[15] sodium cellulose xanthates,[16] cuprammonium hydroxide,[16] dimethylsulfoxide/paraformaldehyde,[17] phosphoric acid,[17] and SO_2/diethylamine/dimethylsulfoxide solution.[18] Moreover, most of these methods either were toxic or inevitably caused degradation of cellulose, which were

disadvantageous for scientific studies and practical application of ACF.

The cellulose solvent of LiCl/*N,N*-dimethylacetamide (DMAc) was first reported by C. L. McCormick and D. K. Lichatowich in 1979.[19] Initially, water swelled and opened the structure; inter and intra-molecular hydrogen bonds were replaced by hydrogen links with H_2O; methanol and DMAc were introduced subsequently to remove water and impede the inter- and intra-hydrogen bonds to re-form; in final step, the swollen sample was added into LiCl/DMAc solvent, stirring until dissolved.[20,21] Although the mechanism of dissolution remained controversial, one generally accepted principle was that $[DMAc_n+Li]^+$ macrocation evolved, leaving the chloride anion (Cl^-) free. Thereby Cl^- was highly active as nucleophilic base and played a major role by breaking up the inter- and intra-hydrogen bonds.[19-24] The whole process was operated under mild condition, and no appreciable degradation occurred. In addition, the cellulose solution in LiCl/DMAc was reported to be extremely stable,[20,21] which made it attractive for practical application. However, only a few reports were related to the preparation of cellulose film from LiCl/DMAc solution.[25-32] On top of that, none of them mentioned the fabrication of ACF.

In this study, ACF with excellent transparency was prepared by regeneration from LiCl/DMAc solution. The relationships between concentration of cellulose solution and the mechanical properties were systematically investigated. We also compared the enzymatic hydrolysis rate of ACF and commercially available Cellophane. This study would provide a simple, less-destructive, and universal method to prepare amorphous cellulose film, in addition, enhance our understanding about behaviors of the amorphous cellulose and open its new practical application.

Experimental section

Materials. Whatman CF11 fibrous medium cellulose powder (CF11, cotton origin, 50-350 μm, GE Healthcare Life Science Corp., Piscataway, NJ, USA),

Microcrystalline cellulose powder (Merck, cotton origin, 20-160 μm, ≥ 80%, Merck KGaA, Darmstadt, Germany), Avicel SF microcrystalline cellulose powder for thin layer chromatography (Avicel, pulp origin, mean particle size around 10 μm, Funakoshi, Co., Ltd., Tokyo, Japan), and bacterial cellulose prepared as described previously except for under static condition (BC, *Gluconacetobacter xylinus* (Brown) Yamada et al. ATCC 53524)[33] were used as cellulose resource. For reference, amorphous cellulose sample derived from CF11 was prepared through vibrating ball-mill in N_2 atmosphere for 48 h by using ceramic balls (Ball-mill, Type MB-1 Vibrating mill, Chuo Kakohki, Co., Ltd., Nagoya, Japan).[13] Cellophane (thickness ≈ 22μm) without any additives and coating was kindly supplied by Futamura Chemical Co., Ltd., Nagoya, Japan. *N, N*-dimethylacetamide (DMAc, purity > 99%) was obtained from Tokyo Chemical Industry Co., Ltd., Japan. Anhydrous lithium chloride (LiCl), D-glucose, anhydrous citric acid, 3,5-dinitrosalicylic acid (DNS), potassium sodium (+)-tartrate tetrahydrate (Rochelle salt), methanol, acetone were obtained from Wako Pure Chemical Industries, Ltd., Japan. Cellulase from *Aspergillus niger* (activity ≥ 60,000 unit/mg) was obtained from MP Biomedicals, LLC., Santa Ana, CA, USA. All reagents without special mention were used as received.

Preparation of cellulose solution. The first step was the fabrication of cellulose solution from different cellulose resources. To facilitate mass production, the reported method[20,21] was simplified (Fig. S1). In a typical run, 3 g CF11 was immersed in deionized water for 4 h at room temperature (RT, 25 °C) and filtered to remove water, followed by successive solvent exchange with methanol and DMAc, each for 2 h. Then, the activated cellulose was soaked in 47 g LiCl (8 wt%)/ DMAc solution with the protection of N_2 atmosphere. After mechanical stirring for 12 h, a clear cellulose solution was obtained. To complete the dissolution of cellulose, the solution was placed overnight at 4 °C.[20] Finally, a transparent cellulose solution with 6 wt% concentration was obtained. The solution was stored at 4 °C until use. For the

concentration below 6 wt%, the solution became clear only after stirring for several hours. With respect to 8 wt%, 24 h were needed for complete dissolution. According to the same procedure, 6 wt% of Merck and 6 wt% of Avicel cellulose solutions were obtained. The dissolution time was less than 2 h for both samples. On the contrary, even for 1 wt% of BC solution, the dissolution took at least 24 h, and the viscosity of solution is higher than other samples.

Preparation of cellulose film. The cellulose solution was degassed by centrifugation at 10000 rpm for 10 min at RT, then casted on a glass plate. The thickness was controlled at 0.5 mm using an applicator. After the glass plate was gently immersed into 100 ml of acetone bath, a transparent cellulose gel immediately formed. The cellulose gel was kept in acetone for 1 h, and washed with 100 ml deionized water for five times to remove the salt completely, each time for 1 h. For preparation of cellulose films, usability of various kinds of organic solvent other than acetone was checked as regeneration solvents; water, methanol, and ethanol. The washed sample was fixed on the poly(methyl methacrylate) (PMMA) plate with adhesive tapes to prevent shrinkage[10] and dried in the oven at 40 °C for 2 h. The glass and Teflon plates were also employed as substrate for this drying process (Fig. S1). The sample was further dried in a desiccator containing phosphorus pentaoxide at RT for at least 48 h. Finally, for 6 wt% of CF11 solution, a transparent cellulose film was obtained with the thickness about 22 μm. In the following content, the samples prepared from different kinds and concentration of cellulose solutions were referred to as CF11 4%, CF11 5%, CF11 6%, CF11 7%, CF11 8%, Merck 6%, Avicel 6%, and BC 1%, respectively.

Enzymatic hydrolysis of CF11 6% and Cellophane. CF11 6% and Cellophane having similar thickness of 22-23 μm were treated with cellulolytic enzymes. Hydrolysis experiments were run concurrently. To minimize the difference in specific area, CF11 6% and cellophane were cut into square shape with the same size about 2 cm × 2 cm. For each film, 150 mg of sample, 10 ml of sodium citrate buffer solution (0.05 M, pH

4.8), and 20 mg of cellulase were added in this order to a 50-ml-vial. The vials were capped and put into a bioshaker at 40 °C with shaking speed 200 rpm. To monitor the content of released reducing sugar, 100 µl of the supernatant was transferred from the vial to a test tube periodically and diluted with 2.9 ml of Milli-Q water, followed by blending with 3 ml of DNS reagent, which was prepared according to the method reported by Miller.[34] The test tubes were heated in a boiling water bath for 15 min. After the development of color, 1 ml of 40 wt% Rochelle salt solution was added immediately. The test tubes were rapidly cooled down to RT by running water. The absorbance of the solution was measured at 575 nm using a Hitachi U2810 UV-visible spectrophotometer. Finally, the released reducing sugar content was calculated as D-glucose.

Characterization. Fourier transform infrared (FT-IR) spectra in the attenuated total reflection (ATR) mode were recorded on a Nicolet iS5 FT-IR Spectrometer with iD5 ATR accessory (Thermo Fisher Scientific Inc., Waltham, MA, USA). The optical transmittances of the films were measured from 200 to 900 nm using a Hitachi U2810 UV-visible spectrophotometer. Scanning electron microscopic (SEM) analysis was carried out by a HITACHI SU-3500 instrument (Hitachi High-Technologies Corp., Tokyo, Japan). Wide-angle X-ray diffraction (XRD) was performed on an X-ray diffractometer (Shimadzu XRD-6100) at a rate of 2° (2θ) min^{-1} over the 2θ range from 5 to 40°. The X-ray radiation used was Ni-filtered CuKα with a wavelength of 0.15406 nm. The voltage and current were set at 40 kV and 30 mA, respectively. Solid-state ^{13}C-NMR spectra with cross polarization/ magic angle spinning (CP/MAS) were recorded on a 600 MHz NMR spectrometer (150.95 MHz for ^{13}C, Advance III, Brucker BioSpin GmbH, Rheinstetten, Germany) at RT. The chemical shift was calibrated by carbonyl carbon of glycine at 176.46 ppm. The cellulose distribution in cellulose films was observed by X-ray computed tomography (XCT) instrument at 80 kV and 100 µA with isotropic voxcel of 600 nm (SKY Scan 1172, High resolution micro-CT, Brucker AXS GmbH, Karsruhe, Germany). Tensile properties were

measured by a Shimadzu EZ Graph instrument equipped with a 500 N load cell (Shimadzu Corp., Kyoto, Japan). A crosshead speed of 1 mm/min was used. The sample was cut into rectangular strips 40 mm × 5 mm and tested with a span length of 10 mm.

Results and discussion

Characterization of cellulose film

To prepare the cellulose film with good appearance, three substrates were employed during the drying process (Fig. S1). The film well attached to the glass plate, but the bonding force between surfaces was so strong that the film could not be pelt off from the plate. In contrast, the bonding force between the film and Teflon was too weak to maintain the shape of the film, which was easily deformed after drying. The best result was obtained by using PMMA plate. The bonding force between the surfaces was strong enough to fix the cellulose film. Meanwhile, the film can be easily detached from the plate. Considering the cost and environmental friendliness, four common solvents, water, methanol, ethanol, and acetone, were chosen as the regeneration solvent. The first three kinds of solvents caused drastic shrinkage of the cellulose film. Only in the case of acetone, however, transparent, flat and smooth cellulose film was obtained. Usability of acetone as a regeneration solvent was previously reported,[10,35] but no description about preparation of transparent films has been noted by using the LiCl/DMAc solvent system. In addition, it was reported that acetone will lead to better amorphous cellulose structure.[18] Based on the above reasons, acetone was chosen as the regeneration solvent. All of cellulose films regenerated individually from CF11, Merck, Avicel and BC cellulose solutions in LiCl/DMAc by acetone possessed good optical appearance. Among them, CF11 6% was taken as a typical example and its photographic appearance was shown in Fig. 1. Smooth and dense surface was observed by SEM in the micron level (Fig. S2). The thickness of cellulose films increased with increasing concentration

of cellulose solution from 4 to 7 wt% (16, 18, 22, and 29 μm, respectively), and slight decrease appeared at 8 wt% (27 μm) because of incomplete dissolution of cellulose into the solvent.

(Insert here Fig. 1)

The crystalline structure of the native CF11, Merck, Avicel and BC samples was studied by XRD (Fig. 2a). The typical diffractions due to I_β rich natural cellulose for the former three were observed at 2θ = 14.8°, 16.3°, and 22.6°, which were corresponding to the $(1\bar{1}0)$, (110), and (200) planes,[36] respectively. In the case of I_α rich BC, three distinct diffractions (100), (010), and (110) were observed at 2θ = 14.6°, 16.9°, and 22.7°, respectively.[33] After regeneration, these diffractions disappeared, showing a broad peak at $2\theta \approx 20°$ (Fig. 2b), which indicated that cellulose I structure was transformed to amorphous cellulose during the dissolution, regeneration and drying process. Compared to Ball-mill cellulose, the regenerated samples showed similar diffractions, except that, for Avicel 6%, there were weak peaks appearing at around 2θ = 12.1° and 22.0°. These diffractions were attributed to cellulose II structure, indicating that a little amount of cellulose II structure was also formed apart from amorphous cellulose.

(Insert here Fig. 2)

The amorphous structure of cellulose films was further confirmed by CP/MAS ^{13}C NMR (Fig. 3). The native cellulose showed characteristic signals assignable to cellulose I (Fig. 3a): the signals around 105 ppm were assigned to the most deshielded anomeric carbon atom C1; the sharp signal at 89 ppm and the broad signal between 86 ppm and 80 ppm were assigned to C4 in crystalline and amorphous region, respectively; the signals from 79 ppm to 70 ppm belonged to C2, C3, and C5; similar to C4, C6 displayed a sharp signal at 65 ppm and a broad signal around 63 ppm, corresponding to crystalline and amorphous region, respectively.[37] After regeneration (Fig. 3b), all signals showed a decrease in sharpness, especially for C4. The sharp peaks at 89 ppm totally

disappeared for CF11 6%. With respect to the other regenerated samples, only two small signals appeared in this area, because of the regeneration of a little amount of cellulose II structure. Meanwhile, the strength of signals from 86 ppm to 80 ppm increased for all samples. These changes stemed from the differences between crystalline and amorphous structure, including conformational differences, differences in bond geometries, non-uniformities of neighboring chain invironments.[38] The results of regenerated samples were similar with ball-milled sample, indicating that highly amorphous cellulose films were obtained. Moreover, for CF11, the transformation from cellulose Ⅰ to amorphous cellulose was more completely achieved by regeneration from the LiCl/DMAc solution, compared to the ball-milling method. Since there were still two small signals around 89 ppm displaying for the ball-milled sample, due to the remaining cellulose Ⅰ structure.

(Insert here Fig. 3)

FT-IR results (Fig. 4) also provided the evidence of transformation from crystalline to amorphous structure. The absorption at 1429 cm^{-1} was assigned to CH_2 symmetrical bending vibration and the absorption at 897 cm^{-1} responded to change in molecular conformation due to rotation about β-(1→4)-D-glucosidic linkage.[39] Normally, these two bands were used to measure the crystallinity of cellulose. In the native cellulose (Fig. 4a), a sharp absorption at 1429 cm^{-1} and a weak band at 897 cm^{-1} appeared. In the regenerated cellulose film (Fig. 4b), on the other hand, only a broad absorption at 1429 cm^{-1} could be seen and the intensity of the absorption at 897 cm^{-1} increased, proving the low crystallinity of regenerated film. In addition, the intensity of other peaks at 1335, 1315, 1111, 1057 and 1033 cm^{-1} decreased after regeneration. The broad absorption in the 3600-3000 cm^{-1}, due to the OH- stretching vibration, could reflect the changes of hydrogen bonds. A narrow peak appeared at 3340 cm^{-1} for native cellulose, which was caused by regular arrangement of intra- and inter- hydrogen bonds. After regeneration, regularity of hydrogen bonds was disturbed, the peak shifts to high

wavenumber 3350 cm^{-1} and broadening were also detected. Since it was reported that unbounded or "free" OH groups absorb infra-red light at 3584 to 3650 cm^{-1},[40] which was higher than observed in the prepared films, we could conclude that hydroxyl groups in amorphous structure existed in an irregular arrangement of hydrogen bonds rather than free mode.

(Insert here Fig. 4)

In conclusion, all of the cellulose samples, that were CF11, Merck, Avicel, and BC, could be transformed from cellulose I to highly amorphous structure. Among of them, the best result was obtained with CF11, whereas there was a little amount of cellulose II structure regenerated in the cases of Merck, Avicel, and BC. Therefore, in the following content, properties of the ACF derived from CF11 were investigated and compared with those of Cellophane.

Mechanism of the formation of ACF

We have attempted to give an explanation about the formation of ACF. Cellulose is mainly composed of two parts, namely, crystalline and disordered regions. In most of cases, the latter is referred to as "amorphous". Compared to amorphous parts, crystalline structure is more difficult to access and is main obstacle for dissolution. First, water is used to swell crystalline lattice, making LiCl/DMAc solvent easy to penetrate. During the dissolution process, the $[DMAc_n+Li]^+$ macrocation is evolved, leaving the chloride anion (Cl^-) free, which disturbs inter- and intra- hydrogen bonds by forming new hydrogen bonds with hydroxyl groups of cellulose chain.[24] After that, cellulose chains become much easier to tear off from crystalline lattice and drag into solution. This process repeated until the "true" solution is formed, in which cellulose chains freely extend unlike in the other kinds of solvents such as the aqueous NaOH/urea.[41] When this cellulose solution is immersed into a poor-solvent, cellulose immediately reprecipitated from the solution through the entanglement of molecular chains, leading

to the formation of cellulose gel. Followed by the drying process, water quickly evaporates accompanying the collapse of the pores in the hydrogel due to the high surface energy of water. In addition, the regeneration of hydrogen bonds between cellulose chains provides another driving force. Finally, the ACF with dense structure was obtained. Although cellulose II is thermodynamically more stable, the drying process is so fast that kinetic control takes advantage, no enough time is left to rearrange cellulose chains, which are more likely aligned in a bent and twisted conformation. A large amount of intra-hydrogen bonds replace the inter-hydrogen bonds existing in native cellulose to stabilized this conformation, making the ACF stable in common conditions unless exposed to high temperature, moisture, or pressure.

It is worthy to mention about the influence of cellulose resources on its solubilization and the formation of amorphous structure. Three plant celluloses with different particle size (CF11 > Merck > Avicel) were chosen. According to XRD (Fig. 2) and ^{13}C NMR (Fig. 3) results, the sequence of the perfection of amorphous structure was CF > Merck > Avicel, consistent with their particle size. To some extent, particle size is related with molecular chain length or degree of polymerization (DP). In the case of Avicel, short chain length causes large specific surface area contactable with the solvent, which promotes their high mobility leading to form thermodynamically favored cellulose II structure during the regeneration and drying process. With respect to BC, because of its distinct complex entangled structure, the solubilization is difficult. Moreover, the viscosity of solution is obviously higher than those of the other three plant cellulose, reflecting the longest chain length of BC among the chosen cellulose resources. Molecular chains of BC probably still remain some extent of orientation in the solubilized state, which easily leads to the formation of crystalline structure. Therefore, only for the sample with median particle size, such as CF11, more perfect amorphous structure could be obtained.

Transparency of CF11 and Cellophane

The transparency of cellulose films was investigated by UV-visible spectroscopy. As shown in Fig. S3, all of the cellulose films from CF11 4% to CF11 8% possessed high transparency not only in the visible region (transmittance is about 90%) but also in near ultraviolet region (transmittance is above 70%), which was better than the commercial Cellophane (Fig. 5) and the other cellulose films reported in the reference.[10,42,43] The reason may be resulted from the difference of crystalline structure between CF11 films and Cellophane, the latter was characterized as cellulose II by XRD (Fig. S6) and ^{13}C NMR spectra (Fig. S7). To further investigate the reason, XCT was measured, which was recently used in cellulose materials area.[44-46] With the help of XCT, a volumetric map of specimen in three dimensions could be obtained. Meanwhile, the distribution of different component and pores could be differentiated. As the XCT images (Fig. 6) showed, CF11 6% was more homogeneous compared with Cellophane in the order of $\geq$ 600 nm. In the latter case, presence of cloudy aggregates that may be composed of the small crystal grains could be clearly detected. Such aggregates would cause the scattering of light, resulting in the inferior transparency of Cellophane.

(Insert here Fig. 5)

(Insert here Fig. 6)

Mechanical properties of CF11 and Cellophane

Tensile properties of cellulose films were investigated. For reference, Cellophane was tested. Fig. 7 shows us the typical stress-strain curves of cellulose samples. Table 1 summarizes the tensile properties of the measured samples. The elongation at break and maximum stress for CF11 4% were 15.9% and 133 MPa, respectively. With the increasing concentration of cellulose solution, the elongation at break increased. After the maximum value 23.9% was obtained for CF11 6%, an obvious decrease was shown for CF11 8% because of incomplete dissolution of cellulose, which was confirmed by the XRD results (Fig. S4). The undissolved grain

will function as defect detrimental to the tensile performance. The largest maximum stress value was about 160 MPa belonging to CF11 5% and CF11 6%. Since CF11 6% and cellophane possess similar thickness, the tensile properties of them were compared. The elongation at break (23.9%) and maximum stress (157 MPa) of CF11 6% were higher than those of cellophane (19.9% and 135 MPa, respectively). Although, the cellulose resource would affect the mechanical properties, such a rarely reported performance is probably attributed to the distinctive amorphous structure of ACF. In amorphous structure, cellulose chains are assumed to be bent and twisted, inter-hydrogen bonds are ripen off and regenerated under stretching, leading to extension and rearrangement of cellulose chain in a regular way, finally higher elongation at break and maximum stress are desirably obtained.

(Insert here Fig. 7 and Table 1)

Enzymatic hydrolysis of CF11 6% and Cellophane

Results of enzymatic hydrolysis of CF11 6% and Cellophane are shown in Fig. 8. In the initial 8 h, the concentration of reducing sugar released by CF11 6% rapidly rose to 3.7 mg/ml, showing a little lower rate in the following time. After 48 h, the concentration increased up to 11.9 mg/ml. Assuming that the released reducing sugar was only comprised of glucose, it can be calculated that about 107 mg of CF11 6% (71.5% of the total amount) was hydrolyzed. Moreover, it was observed that CF11 6% was partially hydrolyzed into small pieces after 48 h. In contrast, the concentration of reducing sugar released by Cellophane rapidly increased to 1.0 mg/ml in the initial 4 h, showing only a little increase to 1.7 mg/ml after 48 h. About 15.0 mg of Cellophane (10.0% of the total amount) was hydrolyzed. In addition, the films remained intact. The enzymatic hydrolysis rate of CF11 6% was above 7 times higher than that of Cellophane. To explain this phenomenon, the mechanism of enzymatic hydrolysis would be focused. Generally, the activity of cellulolytic enzymes largely depends on their types (endo- and

exo-glucanases) and accessibility on the surface of cellulose as subtrate.[47,48] Usually cellulase derived from *Trichoderma* and *Aspergillus* spp. are used for degradation of natural cellulose I and more soft cellulosic materials, respectively. By thinking about amorphous nature of the present films, we selected a cellulase originated from *Aspergillus niger* for testing their biodegradability. For the Cellophane (cellulose II), only cellulose chains on the surface are available for the attachment of the cellulase since cellulose chains stack closely, and the film will be decomposed layer by layer. This process will greatly inhibit the hydrolysis of Cellophane. The rapid increase in the beginning is attributed to the amorphous region in the surface of Cellophane. With respect to CF11 6%, cellulase does not only function on the surface but also acts on internal chains because of more open and accessible structure. Under the similar conditions, CF11 6% will provide more active sites and chain ends for attacking by cellulase. Eventually, CF11 6% shows higher efficiency of enzymatic hydrolysis. Therefore, it is reasonable to conclude that CF11 6% will be decomposed much faster in natural world and have more friendliness to the environment than cellophane or other crystalline type of cellulose products. What's more exciting is that, cellulosic waste derived from ACF film can be recycled and converted to liquid fuels[49] due to its higher efficiency of enzymatic hydrolysis compared to the other cellulose resource, which will completely release the burden to the environment.

(Insert here Fig. 8)

Conclusions

Cellulose films with excellent transparency were regenerated from LiCl/DMAc solutions by using acetone as the regeneration solvent. The cellulose films were highly amorphous, which was confirmed by the XRD, ^{13}C NMR and FT-IR measurements. According to our best knowledge, it was the first time to prepare such amorphous cellulose films with good performance through a simple, less-destructive, and universal

method. Compared with commercial Cellophane, ACF possessed comparable mechanical performance but much faster enzymatic hydrolysis rate due to its distinctive amorphous structure that is more open and accessible, indicating its prevailed environmental friendliness. Based on the present results, we can conclude that the ACF possessed great potential to replace cellophane used as packaging materials. Moreover, it was of important meaning to serve as a new standard sample for the study of cellulose structure and enzyme activity.

Acknowledgement

B.Z. would like to thank China Scholarship Council (CSC) for a scholarship support.

References

1. R. J. Moon, A. Martini, J. Nairn, J. Simonsen and J. Youngblood, *Chem. Soc. Rev.*, 2011, **40,** 3941-3994.
2. M. A. S. Azizi Samir, F. Alloin and A. Dufresne, *Biomacromolecules*, 2005, **6**, 612-626.
3. D. Klemm, B. Heublein, H.-P. Fink and A. Bohn, *Angew. Chem. Int. Ed*, 2005, **44,** 3358-3393.
4. A. C. Osullivan, *Cellulose*, 1997, **4**, 173-207.
5. S. Yano, H. Hatakeyama and T. Hatakeyama, *J. Appl. Polym. Sci.*, 1976, **20**, 3221-3231.
6. R. Rinaldi and F. Schüth, *ChemSusChem*, 2009, **2**, 1096-1107.
7. A. P. Dadi, S. Varanasi and C. A. Schall, *Biotechnol. Bioeng.*, 2006, **95**, 904-910.
8. M. S. Bertran and B. E. Dale, *Biotechnol. Bioeng.*, 1985, **27**, 177-181.
9. L. T. Fan, Y.-H. Lee and D. H. Beardmore, *Biotechnol. Bioeng.*, 1980, **22**, 177-199.
10. Q. Yang, H. Fukuzumi, T. Saito, A. Isogai and L. Zhang, *Biomacromolecules*, 2011, **12**, 2766-2771.
11. H. P. Fink, P. Weigel, H. J. Purz and J. Ganster, *Prog. Polym. Sci.*, 2001, **26**, 1473-1524.
12. H. Qi, C. Chang and L. Zhang, *Green Chem.*, 2009, **11**, 177-184.
13. P. H. Hermans and A. Weidinger, *J. Am. Chem. Soc.*, 1946, **68**, 2547-2552.
14. R. S. J. Manley, *J. Polym. Sci., Part A: General Papers*, 1963, **1,** 1893-1899.
15. A. Jeziorny and S. Kepka, *J. Polym. Sci., Part B: Polym. Lett.*, 1972, **10,** 257-260.
16. R. Jeffries, *J. Appl. Polym. Sci.*, 1968, **12**, 425-445.

17. L. R. Schroeder, V. M. Gentile and R. H. Atalla, *J. Wood Chem. Technol.*, 1986, **6**, 1-14.
18. A. Isogai and R. H. Atalla, *J. Polym. Sci., Part A: Polym. Chem.*, 1991, **29,** 113-119.
19. A. El-Kafrawy, *J. Appl. Polym. Sci.*, 1982, **27**, 2435-2443.
20. A. L. Dupont, *Polymer*, 2003, **44**, 4117-4126.
21. C. L. McCormick, P. A. Callais and B. H. Hutchinson, *Macromolecules*, 1985, **18**, 2394-2401.
22. A. M. STRIEGEL, *J. Chil. Chem. Soc.*, 2003, **48**, 73-77.
23. A. Potthast, T. Rosenau, R. Buchner, T. Röder, G. Ebner, H. Bruglachner, H. Sixta and P. Kosma, *Cellulose*, 2002, **9**, 41-53.
24. T. R. Dawsey and C. L. McCormick, *J. Macromol. Sci., Polym. Rev.*, **30,** 405-440.
25. Y. Nishio and R. S. Manley, *Polym. Eng. Sci.*, 1990, **30**, 71-82.
26. Y. Nishio and R. S. Manley, *Macromolecules*, 1988, **21,** 1270-1277.
27. Y. Nishio, S. K. Roy and R. S. Manley, *Polymer*, 1987, **28**, 1385-1390.
28. X. Zhang, J. Zhu, X. Liu and J. Feng, *Cellulose*, 2012, **19**, 121-126.
29. X. Zhang, J. Zhu and X. Liu, *Macromol. Res.*, 2012, **20**, 703-708.
30. X. Zhang, X. Liu, W. Zheng and J. Zhu, *Carbohydr. Polym.*, 2012, **88**, 26-30.
31. J.-W. Kim, S. Park, D. P. Harper and T. G. Rials, *J. Appl. Polym. Sci.*, 2013, **128**, 181-187.
32. W. Gindl and J. Keckes, *Polymer*, 2005, **46**, 10221-10225.
33. T. Iwata, L. Indrarti and J.-I. Azuma, *Cellulose*, 1998, **5**, 215-228.
34. G. L. Miller, *Anal. Chem.*, 1959, **31**, 426-428.
35. H. Geng, Z. Yuan, Q. Fan, X. Dai, Y. Zhao, Z. Wang and M. Qin, *Carbohydr. Polym.*, 2014, **102**, 438-444.
36. A. Isogai, M. Usuda, T. Kato, T. Uryu and R. H. Atalla, *Macromolecules*, 1989,

22, 3168-3172.

37. R. H. Atalla, J. C. Gast, D. W. Sindorf, V. J. Bartuska and G. E. Maciel, *J. Am. Chem. Soc.*, 1980, **102**, 3249-3251.

38. D. L. VanderHart and R. H. Atalla, *Macromolecules*, 1984, **17**, 1465-1472.

39. M. L. Nelson and R. T. O'Connor, *J. Appl. Polym. Sci.*, 1964, **8**, 1311-1324.

40. T. Kondo and C. Sawatari, *Polymer*, 1996, **37**, 393-399.

41. J. Cai and L. Zhang, *Macromol. Biosci.*, 2005, **5**, 539-548.

42. A. N. Nakagaito, M. Nogi and H. Yano, *MRS Bulletin*, 2010, **35**, 214-218.

43. M. Nogi, S. Iwamoto, A. N. Nakagaito and H. Yano, *Adv. Mater.*, 2009, **21,** 1595-1598.

44. J. Kastner, B. Plank and D. Salaberger, 18 World Conference on Nondestructive Testing, Durban, 2012

45. J. Kastner, R. Kickinger and D. Salaberger, *J. Cell. Plast.*, 2011, **47**, 567-578.

46. M. Faessel, C. Delisée, F. Bos and P. Castéra, *Compos. Sci. Technol.*, 2005, **65**, 1931-1940.

47. Y.-H. P. Zhang and L. R. Lynd, *Biotechnol. Bioeng.*, 2004, **88**, 797-824.

48. T. T. Teeri, *Trends Biotechnol.*, 1997, **15**, 160-167.

49. E. A. Bayer, R. Lamed and M. E. Himmel, *Curr. Opin. Biotechnol.*, 2007, **18**, 237-245.

455 Table 1 Tensile properties of ACFs and cellophane.

	ACF 4%	ACF 5%	ACF 6%	ACF 7%	ACF 8%	Cellophane
Elongation	15.9	20.7	23.9	22.5	17.6	19.9
(%)	±1.1*	±1.2	±3.2	±2.2	±3.3	±3.7
Max stress	132	161	157	145	145	135
(MPa)	±7	±8	±8	±9	±9	±6

456 *Standard deviation (SD). For each group experiment, 10 samples were tested and at
457 least 3 samples were chosen.

458 **Figure caption**

459 Figure 1 Photo of transparent film of CF11 6%.

460 Figure 2 X-ray diffractions of (a) native samples, (b) regenerated samples and
461 ball-milled sample.

462 Figure 3 CP/MAS ^{13}C-NMR spectra of (a) native samples, (b) regenerated samples and
463 ball-milled sample.

464 Figure 4 FT-IR spectra of (a) native samples, (b) regenerated samples and ball-milled
465 sample.

466 Figure 5 Transmittance of CF11 6% and Cellophane at UV-visible wavelength region.

467 Figure 6 X-ray CT image of (a) CF11 6% and (b) Cellophane.

468 Figure 7 Stress-strain curves of CF11 6% and Cellophane.

469 Figure 8 Time course of enzymatic degradation of CF11 6% and Cellophane.

Figure 1 Photo of transparent film of CF11 6%

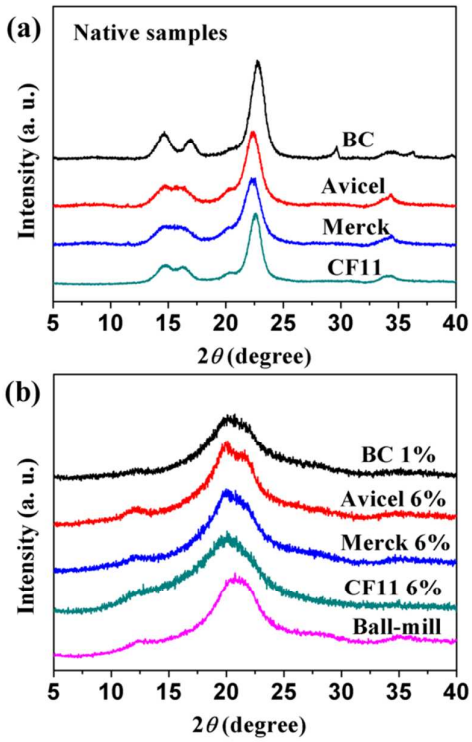

Figure 2 X-ray diffractions of (a) native samples, (b) regenerated samples and ball-milled sample

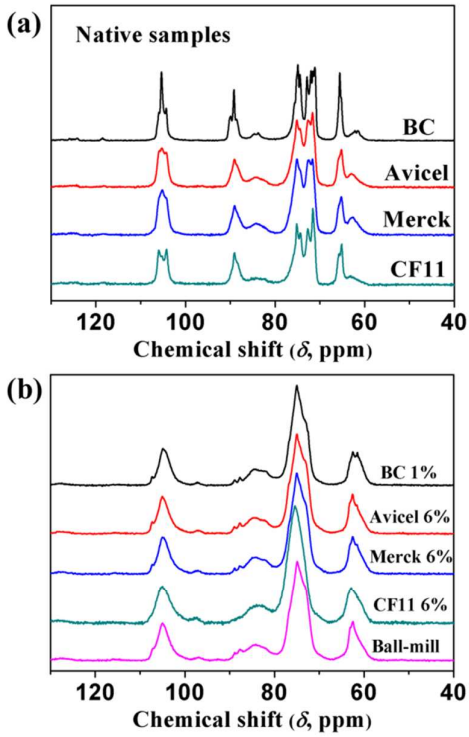

Figure 3 CP/MAS ^{13}C-NMR spectra of (a) native samples, (b) regenerated samples and ball-milled sample

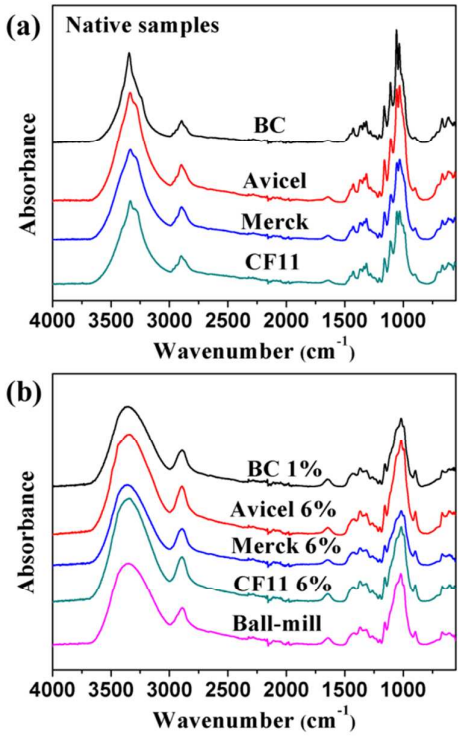

Figure 4 FT-IR spectra of (a) native samples, (b) regenerated samples and ball-milled sample

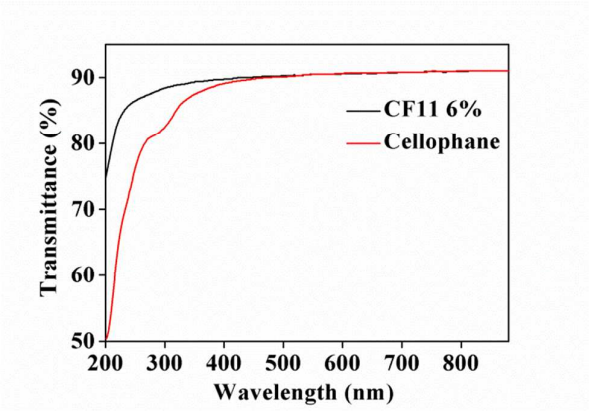

Figure 5 Transmittance of CF11 6% and Cellophane at UV-visible wavelength region

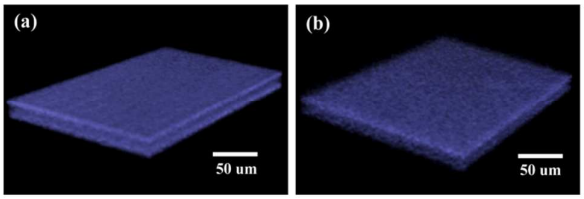

Figure 6 X-ray CT image of (a) CF11 6% and (b) Cellophane

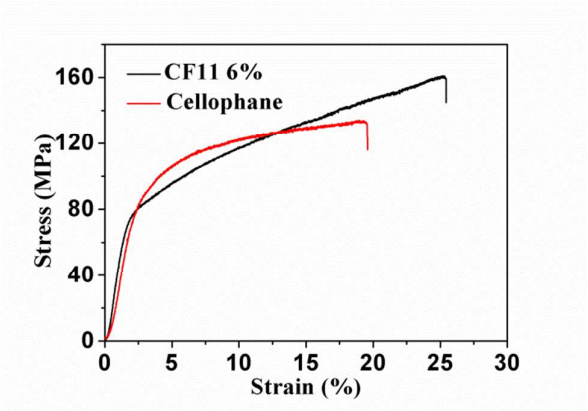

Figure 7 Stress-strain curves of CF11 6% and Cellophane

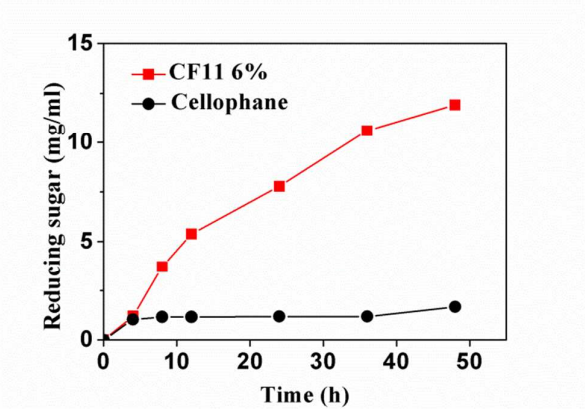

Figure 8 Time course of enzymatic degradation of CF11 6% and Cellophane